Investigating hydrodynamics and turbulent effects in rivers for different flow conditions using spatial complexity metrics

Farhad Bahmanpouri[1], Donatella Termini[2,3], Silvia Barbetta[4], Carlo Gualtieri[5], Marco Dionigi[6], Tommaso Moramarco[7]

(1) Research Institute for Geo-Hydrological Protection, National Research Council (CNR), 06128 Perugia, Italy. Email: farhad.bahmanpouri@irpi.cnr.it
(2) Dipartimento di Ingegneria, University of Palermo, Viale delle Scienze, 90128 Palermo, Italy. Email: donatella.termini@unipa.it;
(3) NBFC, National Biodiversity Future Center, Palermo 90133, Italy
(4) Research Institute for Geo-Hydrological Protection, National Research Council (CNR), 06128 Perugia, Italy. Email: silvia.barbetta@irpi.cnr.it
(5) University of Napoli Federico II, Napoli 80125, Italy. Email: carlo.gualtieri@unina.it
(6) Research Institute for Geo-Hydrological Protection, National Research Council (CNR), 06128 Perugia, Italy. Email: marco.dionigi@irpi.cnr.it
(7) Research Institute for Geo-Hydrological Protection, National Research Council (CNR), 06128 Perugia, Italy. Email: t.moramarco@irpi.cnr.it

Abstract

In non-uniform river flows, hydrodynamic features, such as gradients of velocity in flow directions, are of particular importance for explaining the abundance of aquatic habitats. Hydraulic complexity metrics referred to as M_1, M_2, and M_3 play an important role when it comes to the analysis of habitat metrics on a 3D spatial level. Parameter M_1 is proportional to the drag force experienced by an organism, parameter M_2 represents how much more energy an organism must expend if it moves from the lower velocity to the higher velocity location, and parameters M_3 illustrates the circulation in flow. The specific aim of the present study is to apply those parameters to characterize, under different flow conditions, the cross-sectional distribution of kinetic energy and coherent structures which are both relevant for many aquatic organisms. To this aim, laboratory data as well as field observations along Tiber River, in central Italy, were considered and the hydraulic complexity metrics were investigated in dimensionless form. On the laboratory-scale, the dimensionless parameters M_1^*, M_2^* and M_3^* identify the velocity gradient related to the high/low cross-sectional velocity and the high/low vorticity areas in selected cross-sections along the flume. Then, the evaluation of the parameter M_2* in the horizontal plane allows to verify the relation between the localization of the high/low kinetic energy areas in the

longitudinal direction. For the field-scale, the parameters were investigated, under high, moderate and low flow conditions, in a gauged site in the Tiber River. The results indicate that an aquatic organism should spend more energy where M_3^*, which is related to flow circulation, assumes high values. Furthermore, significant values of M_1^* and M_2^* are observed, which are linked to gradients in the cross-sectional distribution of velocity. These values are predominantly found at the river centerline for M_1^* and at the banks for M_2^*. In terms of echo-hydraulics, the results based on both laboratory and field data indicate that they are complementary, showing that for the larger magnitudes of M_1 and M_3, which are related to the kinetic energy and flow circulation, respectively, an aquatic organism should spend more energy in these zones. Overall, the results based on both laboratory and field studies suggest that parameters M_1 and M_2 are inversely linked, i.e., M_1 decreased with increasing M_2, while, there is no relationship between parameters M_3 and M_1. The findings of the present research would be of particular interest in quantifying biologically important flow patterns occurring at different spatial scales within different streams and under different flow conditions.

Keywords: Hydraulic complexity, Eco-hydrology, Eco-hydraulics, River hydrodynamics, Tiber River.

1. INTRODUCTION

As the physical habitat of in-stream biota, the in-stream habitat is comprised of the channel's physical structure as well as the spatial and temporal dynamics of the flow regime (Maddock 1999). Various in-stream and topographic variables affect habitat structure, including bed slope and deformation, near-bed velocity, and flow circulations (Pedersen et al. 2004). Sustaining biodiversity is essential to the health of our environment and to the quality of human life. For our survival, we are dependent on a variety of aquatic plants, organisms, and their ecological processes. Aquatic biodiversity depends on some factors including a) chemical variables of water quality including factors such as pH, dissolved

oxygen, nutrient levels, and pollutants, b) water temperature, c) the structure and complexity of aquatic habitats, such as the presence of rocks, vegetation, or other physical features, d) availability of foods, e) the connectivity of aquatic habitats to other ecosystems, such as wetlands, rivers, or oceans and f) hydrodynamics of flow including velocity and discharge (J. Morin and McGrady-Steed, 2004; Irfan and Alatawi, 2019; Protasov, et al., 2019). In this direction, the current research, in terms of eco-hydraulic, aims to investigate the hydrodynamic features of flow that affect aquatic organisms. Previous literature studies (Crowder and Diplas 2000, 2002; Gualtieri et al., 2017, 2020) indicated that the hydraulic complexity parameters, M_1 and M_2, provide a description of the magnitude of drag forces applied by aquatic organisms when they move between two locations. The first parameter, M_1, represents the spatial alteration in the flow's kinetic energy. This parameter is defined as a quantitative measure of the extent of power exerted in the process of transitioning from one specific location to another. The second parameter, referred to as M_2, functions as a gauge to determine the additional amount of energy an organism is required to expend when it moves from a region with a lower velocity to one with a higher velocity magnitude. The third parameter, M_3, provides information about circulation zones in the flow which could be potential feeding places for aquatic organisms such as fishes. Overall, with these three parameters, M_1, M_2, and M_3, it becomes possible to assess the hydraulic conditions that are conducive to the existence of an aquatic habitat. Aquatic habitat is extremely dependent upon the spatial heterogeneity and variability of flow characteristics, i.e. water depth and flow velocity. As an example, some researchers (Fausch and White 1981; Rempel et al. 1999) showed that flow patterns, eddies, transverse flows, velocity gradients, and thus turbulent kinetic energy, and other complex hydraulic characteristics can predict salmonid density (Smith et al. 2006). The natural streams were modeled using commercial packages such as River2D, which is a two-dimensional, depth-averaged hydrodynamic model (Blackburn and Steffler, 2002; Clark et al. 2008).

Tritico and Hotchkiss (2005) proved that natural boulders create vertical vortex structures downstream of gravel-bed streams based on spatial variations in bed roughness. Vertical vortices create areas of high and low pressure within the water column which can impact aquatic organisms and river ecology by creating flow circulation zones. This impact can be quite complex and can vary depending on several factors, including the size and strength of the vortex, the geometry of the river channel, and the local topography. As an example, Blettler et al. (2016) verified that the macroinvertebrate diversity increased strongly downstream of the Bermejo and Paraguay River junction. Gualtieri et al. (2017, 2020) investigated the hydraulic complexity parameters through the junction of Negro and Solimões rivers on the Amazon River in Brazil and determined that helical cells forming at the confluence directly affect the flow rotation strength. Nepf et al. (2022) reported a review of some research works on the influence of hydraulic conditions on habitat selection and migration of fish and macroinvertebrates. They reported how habitat selection and swimming patterns are induced by velocity, turbulence, and bed shear stress. Golpira et al. (2022) experimentally investigated the effect of rock-ramp boulder placement with varying boulder concentration and flow rate on habitat hydraulic complexity metrics, including the kinetic energy gradient and modified recirculation metrics. They found that boulder placement with the highest boulder concentration resulted in the greatest habitat hydraulic complexity. Bahmanpouri et al. (2023) analyzed the hydraulic complexity parameters M_1 and M_2 based on laboratory and field data to investigate the drag forces applied by aquatic organisms.

The present study, as continuation of Bahmanpouri et al.' (2023) work, aims to investigate the three hydraulic complexity parameters (M_1, M_2, and M_3) in more detail. These parameters are of particular importance to determining the diversity of aquatic organisms based on analysing the kinetic energy and vorticities at the potential habitat zones. In the pursuit of this endeavour, it is imperative to consider both laboratory-based and field-based

120 measurements, as they provide valuable insights into the development and validation of
121 spatial metrics that are of essential importance in the realm of various stream conditions.
122 The current research endeavours to establish a correlation between energy gradients,
123 vorticity, and flow complexity, all of which play a crucial role in the comprehensive study of
124 aquatic organisms within the context of eco-hydraulics. This study encompasses fishes
125 belonging to diverse species and encompassing different stages of their life cycle. Thus, in
126 the present research, data from both laboratory flume and the field, collected at a gauged
127 section along the Tiber River, in central Italy, under different flow conditions are used. In
128 particular, the analysis of laboratory data has allowed us to isolate the effects of the bed
129 deformation and turbulence structures periodicity, which strongly influence the aquatic
130 habitat, on stream parameters evaluation. Different cross-sections within each of the flow
131 patterns of interest are calculated and scrutinized to examine the considered metrics. The
132 paper is organized as follows: the first Section introduces the laboratory setup and field site,
133 while the second Section describes the theory behind the hydraulic complexity parameters.
134 In Section 3, the results from both laboratory and field data are presented. The paper is
135 ended with the conclusion in Section 4.
136

137 **2. Spatial metrics for river flow complexity: theoretical background**

138 The velocity gradient is a prominent component in a spatially varying flow pattern. It is worth
139 noting that velocity gradients exist near banks, boulders, and other obstructions and are
140 potentially applicable parameters for quantifying and distinguishing between flows having
141 similar depth and velocity values but influenced by different spatially varying flow patterns
142 (Figure 2). Two parameters that address local velocity gradients are defined as potential
143 habitat metrics and they are inferred as (Crowder and Diplas 2000, 2002; Gualtieri et al.,
144 2017; 2020):

145 $$M_1 = \frac{\partial}{\partial s}\frac{V^2}{2} = V\frac{\partial V}{\partial s} \cong V_{ave}\frac{V_2 - V_1}{\Delta_s} \qquad [1]$$

$$M_2 = \frac{\frac{\partial}{\partial s}\frac{V^2}{2}}{\frac{V^2}{2}} \cong \frac{\frac{1}{2}\left(\frac{V_2^2 - V_1^2}{\Delta_s}\right)}{\frac{V_{min}^2}{2}} = \frac{2V_{ave}\frac{V_2 - V_1}{\Delta_s}}{V_{min}^2} \quad [2]$$

where V is the velocity and V_1 and V_2 are magnitudes of velocity between the two consecutive velocity points 1 and 2, whose distance is Δ_s, V_{ave} is the average of V_1 and V_2; V_{min} is the minimum value of V_1 and V_2. The distance Δ_s can be defined in the transverse direction as Δ_y (for the present work Δ_y = 0.07 and 1.0 m for the laboratory and field data, respectively). The first parameter M_1 represents the spatial change in a flow's specific kinetic energy (i.e. per unit mass and unit length [J/Kgm]). The second parameter M_2 scales the spatial change in the kinetic energy of the flow at the point having the lower velocity magnitude.

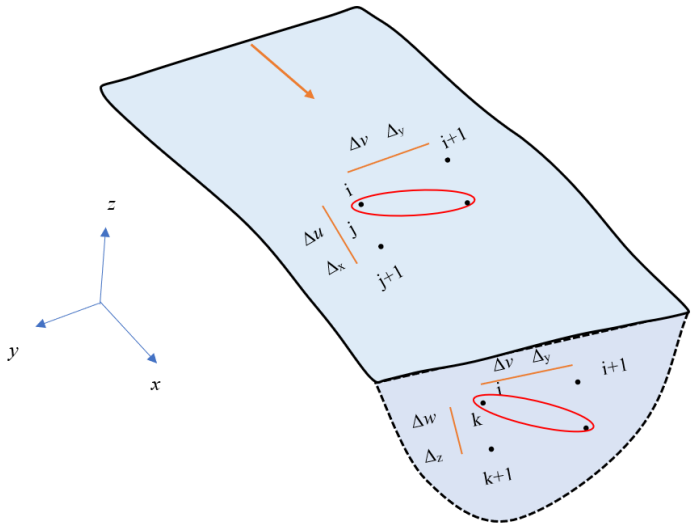

Figure 1. Calculation mesh, *i* in transverse direction, *j* in streamwise direction and *k* in the vertical direction. Red circles show the selected points of velocity in two perpendicular directions

Thus, to distinguish between flows with similar water depth and velocity values but different velocity gradients surrounding them, the parameters M_1 and M_2 allow the evaluation of a flow's velocity gradient and its scaled specific kinetic energy, respectively. In other words, based on Crowder and Diplas (2000), the first parameter (M_1) is proportional to drag force on an organism and it is a measure of the amount of power expended in moving from one

location to another. The second parameter (M_2) represents how much more energy an organism such as fish must expend if it moves from the lower velocity to the higher velocity location. The concept of hydraulic complexity parameters considering the aquatic organisms is highlighted in Figure 2.

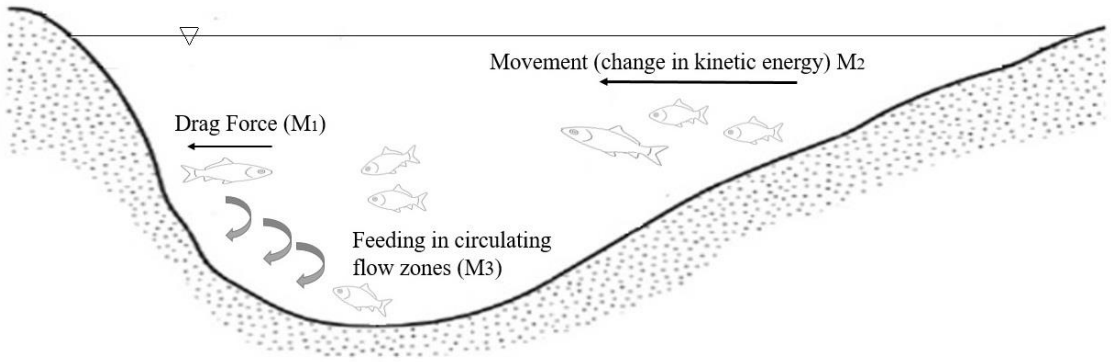

Figure 2. Description of the hydraulic complexity parameters, updated based on Bahmanpouri et al. (2023) to consider M_3

For the first parameter, kinetic energy per unit mass ($\frac{V^2}{2}$) multiplied by a drag coefficient and a frontal area provides the drag force acting on a specific object or organism such as fish (Munson et al., 1990). Hayes and Jowett (1994) and Fausch and White (1981) presented some data to estimate the minimum and maximum possible values of $2V_{ave} \times |(V_2 - V_1)/\Delta s|/V_{min}^2$ that existed at the location of an aquatic organism such as fish. Further, they reported a range of focal point velocity values (V_{min}), "velocity shears" and "velocity differences" that existed at fish locations.

The third parameter M_3 highlights the weighted average of flow rotation in the transversal vertical or horizontal plane, known as ''modified circulation". This parameter is a scale of the strength and frequency of eddies and is defined, in the vertical plane, as (Gualtieri et al. 2020):

$$M_3 = \frac{\int \overline{\int}_s |\xi| \Delta A}{A_{TOT}} = \frac{\sum \left| \left(\frac{\Delta w}{\Delta_y} - \frac{\Delta v}{\Delta_z} \right| \right.}{\sum \Delta_y \times \Delta_z} \times \Delta_y \times \Delta_z \qquad [3]$$

where Δw, Δv and Δu are the variations of velocity in the vertical, transverse and streamwise directions, respectively. Figure 2 depicts the meshing diagram of M_3, which can be calculated in both vertical and horizontal planes, respectively. The M_3 parameter represents the flow circulation within an area, which is important for evaluating the environmental impact of turbulence structures. According to the data by Shields and Rigby (2005), the approximate range of observed magnitudes in the field for the three selected parameters M_1, M_2 and M_3 is 0-0.2 $J.kg^{-1}.m^{-1}$, 0.9-1.3 m^{-1}, 0.2-1 s^{-1}, respectively.

For the present work, the aforementioned parameters are investigated in dimensionless form, i.e. $M_1^* = (M_1-M_{min})/(M_{max}-M_{min})$, $M_2^* = (M_2-M_{min})/(M_{max}-M_{min})$, and $M_3^* = (M_3-M_{min})/(M_{max}-M_{min})$. By employing these dimensionless representations, the collected data can be more effectively compared and analyzed, without losing their meaning.

3. Experimental- and field-scale studies and dataset

3.1 Laboratory-scale data

The laboratory data were collected at the hydraulic laboratory of the University of Palermo (Italy) in research (Termini and Sammartano, 2008; Termini, 2015) aimed to evaluate the flow velocity field and the evolution of turbulent flow structures in a straight flume (see Figure 3). The channel was of width B = 40 cm with fixed banks and bed of quartz sand (D_{50} = median sediment diameter = 0.65 mm). For the purposes of the present work, two runs with flow discharge of 0.013 m^3/s (see also in Termini, 2015) are considered for the analysis: the “Smooth Banks” (“SB”) run, characterized by flat and rigid bed (i.e. the so-called pre-deformed-bed configuration), and the “Deformed Banks” (“DB”) run, which is a mobile-bed run with the same hydraulic conditions as the SB run. The run time was based on the reaching the equilibrium deformed-bed configuration. During the SB run, the 3D instantaneous flow velocity components were measured in 14 points along 5 verticals of 17 measurement cross-sections (sections A ÷ S in Figure 3a). At the end of the DB run, the

bed was found covered by alternating regions of scour-holes/deposit-fronts, as for example Figure 3b shows in the channel reach between sections D and H. In the present work, the analysis is restricted to the channel reach D÷H where the alternating scour-deposit regions were clearly distinguishable.

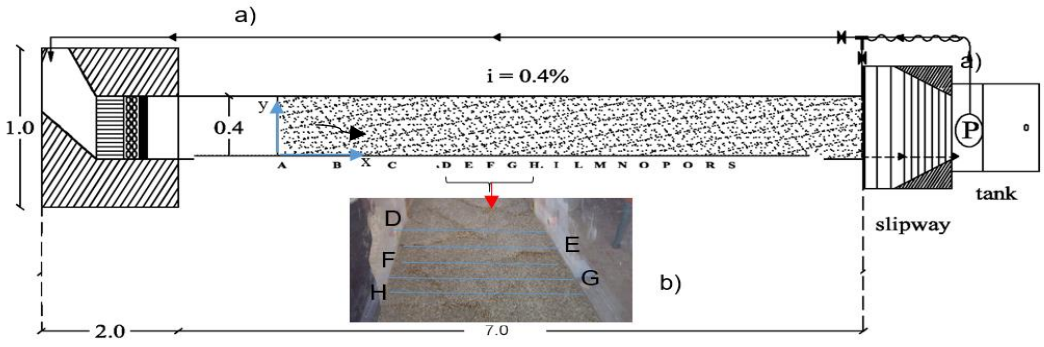

Figure 3. a) Plane-view of the laboratory channel; b) Bed deformation at the end of DB run.

The examined sections D÷H were reciprocally distant of 20 cm so that the channel reach was 80 cm long. As Figure 3b shows, in section D a scour hole is found on the right side of the cross section and a front of deposit formed on the left side. In section E, a new scour hole starts on the right and the left sides. In section F, the bed configuration is similar to that observed in section D. In sections G and H, a front of deposit is found in the central part of the cross-section and two scour holes formed in the left and right sides of the cross-section, almost symmetrically with respect to the channel axis (more details can be found in Termini and Sammartano, 2008; Termini, 2015).

3.2. Field-scale case studies

3.2.1. Upper Tiber River (central Italy)

The Upper Tiber River basin is bounded downstream by the hydrometric section of Ponte Nuovo, with a length of about 120 km from the springs and a drainage area equal to 4145 km^2 (Figure 4).

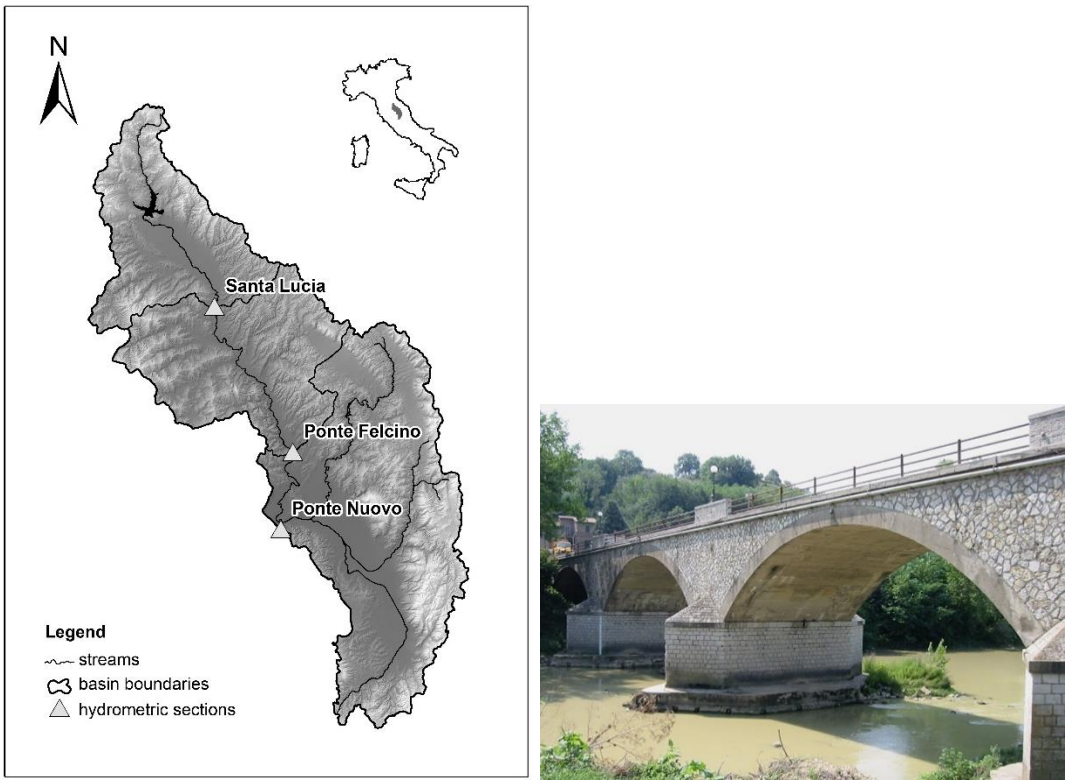

Figure 4. Location of the study area

In this work, the streamwise flow velocity measurement were carried out using an ADCP (acoustic Doppler current profiler) at Ponte Nuovo gauged section. Specifically, a total of three flow measurements were made under different hydraulic conditions, classified as low, medium, and high in Table 1.

Table 1. Main characteristics of the flow velocity measurements used for the analysis at Ponte Nuovo site (Upper Tiber River, central Italy).

Date (flow condition)	River width (m)	Maximum water depth (m)	Aspect ratio (width/depth)	Discharge (m^3/s)
Oct. 2014 (Low flow)	46.7	1.23	37.97	13
Jan. 2015 (Medium flow)	47.27	1.76	26.86	30
Mar. 2015 (High flow)	49.98	2.72	18.38	103

4. Results and Discussion

4.1 Laboratory-scale case

248 The dimensionless parameters M_1^*, M_2^*, and M_3^* are first estimated by using the data
249 collected in sections D÷H of the laboratory channel during the SB run. In a previous work
250 (Bahmanpouri et al., 2023), the analysis of the gradient of the streamwise velocity in
251 sections D and E allowed us to verify that M_1 and M_2 adequately indicate the spatial
252 variation of the kinetic energy due to the alternating high/low velocity pattern in the
253 streamwise direction. In the present work, all the parameters M_1^*, M_2^*, and M_3^* are analyzed
254 in sections D÷H. As Figure 4 shows, while in section D higher values of flow velocity are
255 found on the right side of the cross-section with peak values at Y/B = 0.32, in section E
256 higher values of flow velocity occur almost symmetrically to the channel axis at a relative
257 distance Y/B = 0.32 from the banks. In section F, the distribution of flow velocity is similar to
258 that observed in section D but with lower peak values. In section G, and then especially in
259 section H, the higher values of flow velocity are found almost symmetrically to the channel
260 axis at a relative distance of 0.32 from the banks. In the last two sections, the velocity
261 values are lower than those obtained in sections D÷F. According to findings obtained by
262 Termini (2015) (see also in Termini and Sammartano, 2008), by comparing the distributions
263 of flow velocity shown in Figure 5 with the bed deformation obtained at the end of the DB
264 run (see Figure 3b), it is clear that the higher values of flow velocity occur in the
265 correspondence of the scour holes obtained in the deformed-bed condition.

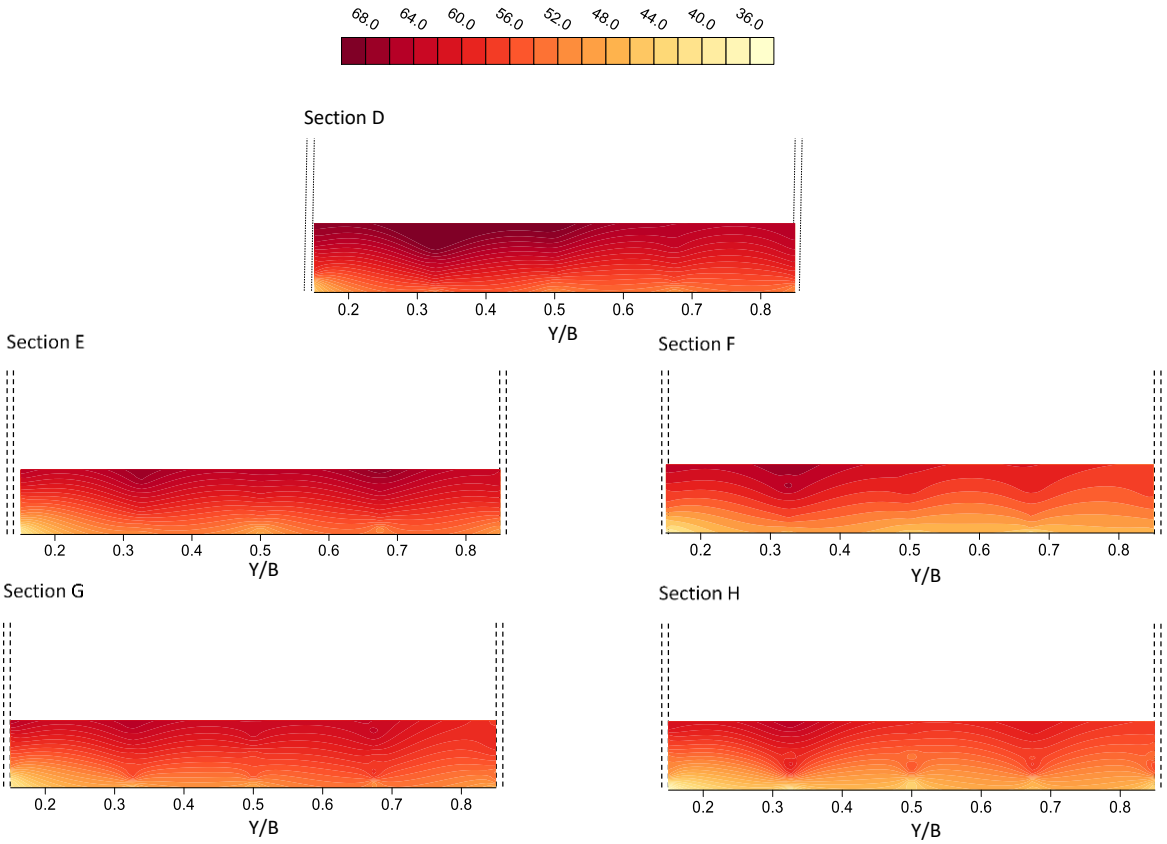

Figure 5. Distribution of the flow velocity V [cm/s] in sections D÷H

Termini (2015) demonstrated that the deformed-bed configuration is strongly related to the formation of alternating regions of high/low flow velocity in the pre-deformed configuration. Figures 6 and 7 report the distributions of the parameters M_1^* and M_2^* estimated in sections D÷H. Figure 6 indicates that in section D, a high spatial velocity gradient (M_1^*) occurs on the right side of the cross-section, reaching its peak value at a relative distance around of 0.3 from the bank. In section E, higher values of M_1^* are found both close to the bed at the right bank and close to the free surface on the left side of the cross section, while in section F, the peak values are observed on the right side of the cross section.

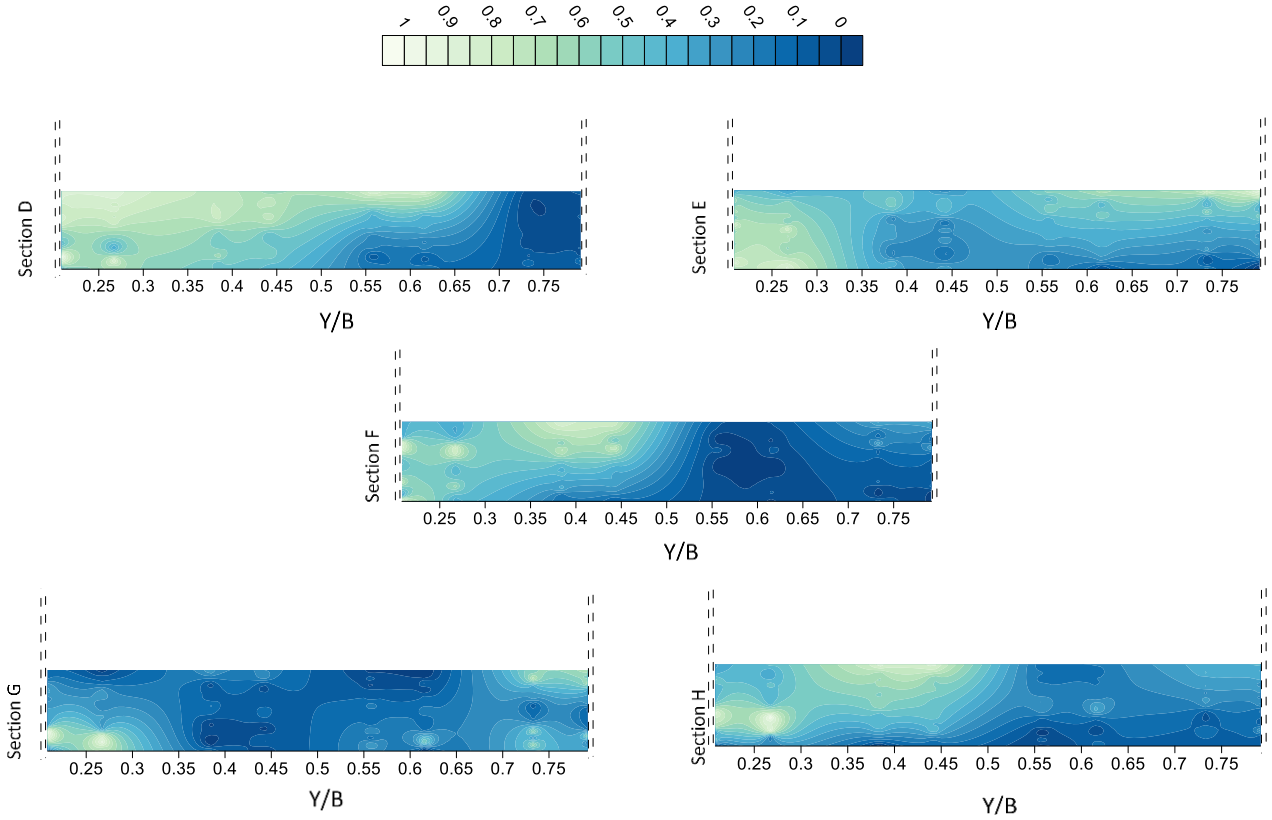

a) Vertical distribution for each section

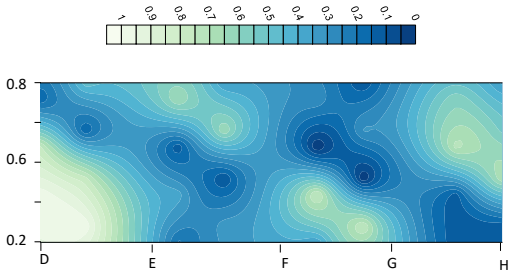

b) Depth-averaged distribution considering all sections

Figure 6. Distribution of the parameter M_1^* in sections D÷H.

Then, in section G, the parameter M_1^* assumes values lower than in the previous sections with higher values close to the bed in both sides of the cross-section. These areas of high values of M_1^* are then extended towards the free surface in section H.

Figure 6 shows the distribution of M_2^* in sections D÷H. The higher values of M_2^* are found on the right side of section D with a peak value close to the bed. Passing from section D to section F higher values of M_2^* are found close to the right bank and including an area

gradually smaller. In section G, two small areas with high values of M_2^* are observed close to the banks. These areas of high values of M_2^* are expanded in the whole water depth in section H.

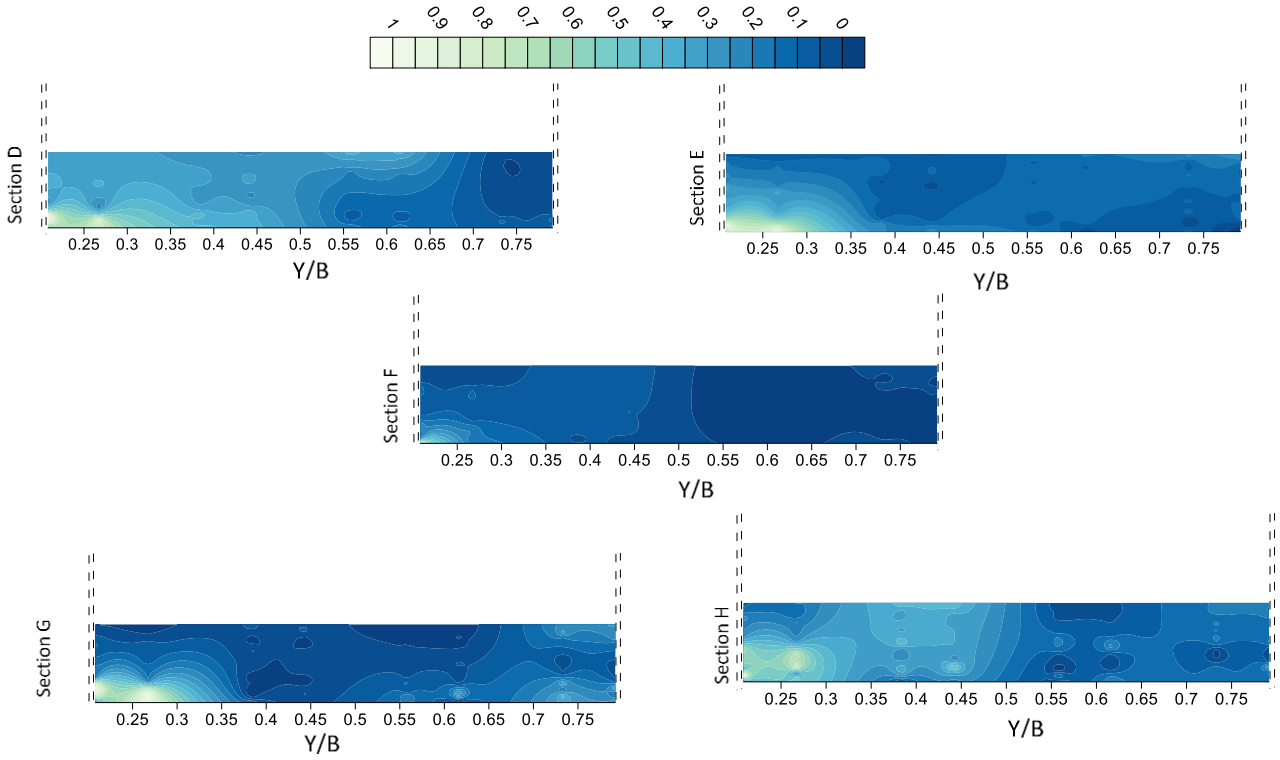

a) Vertical distribution for each section

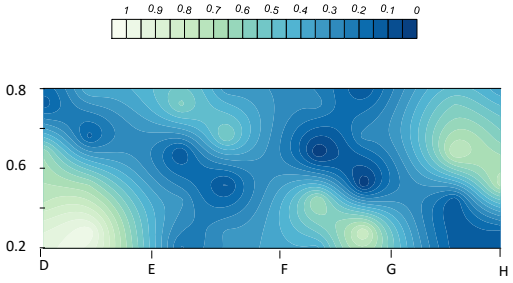

b) Depth-averaged distribution considering all sections

Figure 7. Distribution of the parameter M_2^* in sections D÷H.

The distribution of the parameter M_3^* in sections D÷H is reported in Figure 8. Alternated zones characterized by high/low vorticity values are found. In particular, section D shows high values of M_3^* close to the bed and in the central part (i.e. in the range 0.35 < Y/B <

0.65) where the bed profile changes. This behaviour is also observed in section E, where higher values of M_3* are especially observed moving from the right side towards the left side of the cross-section. In section F, small zones of high circulation can be observed especially at the bed close to both banks and peak values can be also observed near the free surface. In sections G and H, the zones of high circulation close to the bed tend to expand towards the free surface, almost symmetrically to the channel axis.

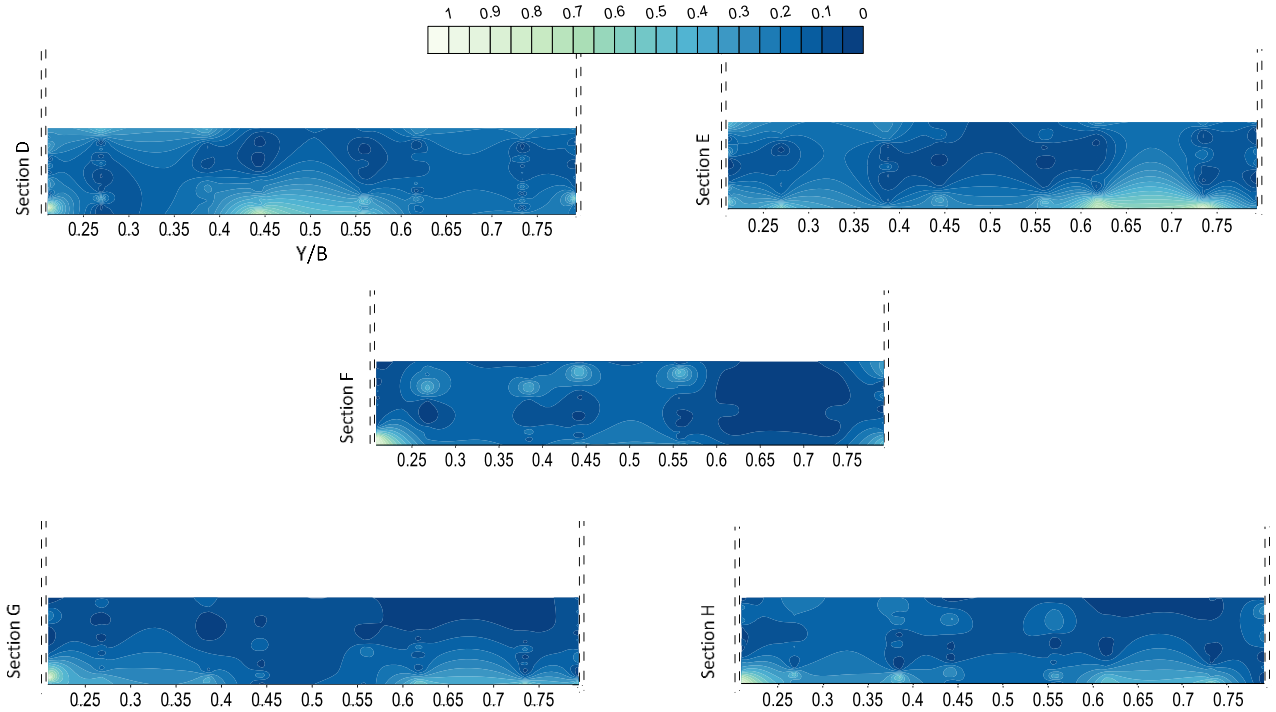

c) Vertical distribution for each section

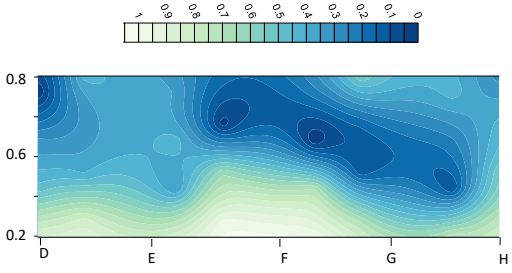

d) Depth-averaged distribution considering all sections

Figure 8. Distribution of the parameter M_3* in sections D÷H.

To examine the relationship between the observed patterns of the parameters M_1* and M_2* and the alternating high/low velocity pattern along the analyzed channel reach, Figure 9 illustrates the horizontal distribution of the depth-averaged velocity V in the reach D÷H. As Figure 9 shows, a high peak of flow velocity occurs near the right bank of sections D and F while lower peak values occur almost symmetrically to the channel axis in sections E and G. In section H such a behavior is maintained although it is less evident and with velocity values lower than those obtained in the upstream sections.

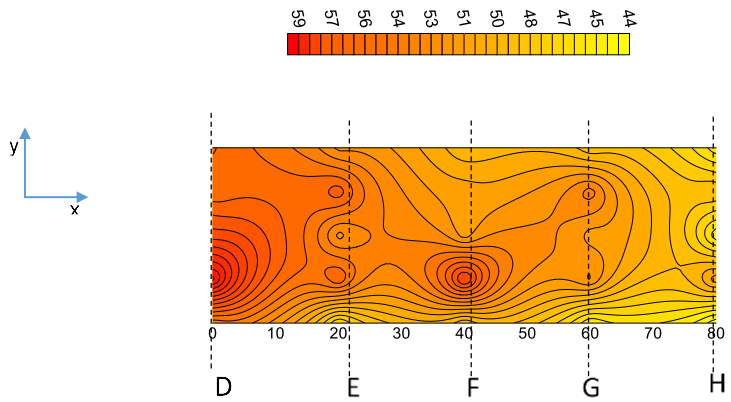

Figure 9. Distribution of the resultant depth-averaged velocity V (cm/s) in the horizontal plane

Figure 10 reports the depth-averaged velocity, V, normalized by the mean velocity Um (with Um=Q/A), and the depth-averaged values of parameters M_1^*, M_2^* and M_3^* in sections D÷H. This figure illustrates that in section D, M_1* decreases passing from the right bank to the left bank. The parameter M_2^* assumes high values for relative distances from the right bank ranging from Y/B=0.25 and Y/B=0.6, where the aquatic organism should spend the higher energy. The flow circulation, given by the parameter M_3^*, assumes an increasing trend passing from Y/B=0.25 cm to Y/B=0.4 and then it decreases assuming a low value at Y/B=0.6, then it increases again. In section E, the depth-averaged value of M_1^* has a decreasing trend on the right side of the cross-section assuming the lowest value at Y/B= 0.4, then it increases until it peaks around Y/B=0.60. The depth-averaged of M_2^* has a

similar trend but it assumes high values in the range 0.25 <Y/B<0.4. The depth-averaged value of M_3^* decreases from the right bank to the transversal abscissa Y/B=0.55; then it increases assuming a high value at Y/B=0.65. In section F, while M_1^* and M_2^* are like in section D, M_3^* decreases on the left side of the cross-section more largely than in section D. In section G, the values of M_1^* in the right side of the cross-section are lower than those observed in section F assuming the lowest value at Y/B=0.4 then, it slightly increases. The values of M_2^* assume a behaviour similar to M_1^*. M_3^* decreases from the right bank to the channel axis where it reaches a minimum value; then it increases again. Lastly, in section H, both M_1* and M_2* have higher values in the range at 0.25 <Y/B<0.4, then they decrease assuming the lower value at Y/B=0.55 cm and then they increase again. Additionally, the magnitude of M_3* decreases with increasing the distance from the right bank.

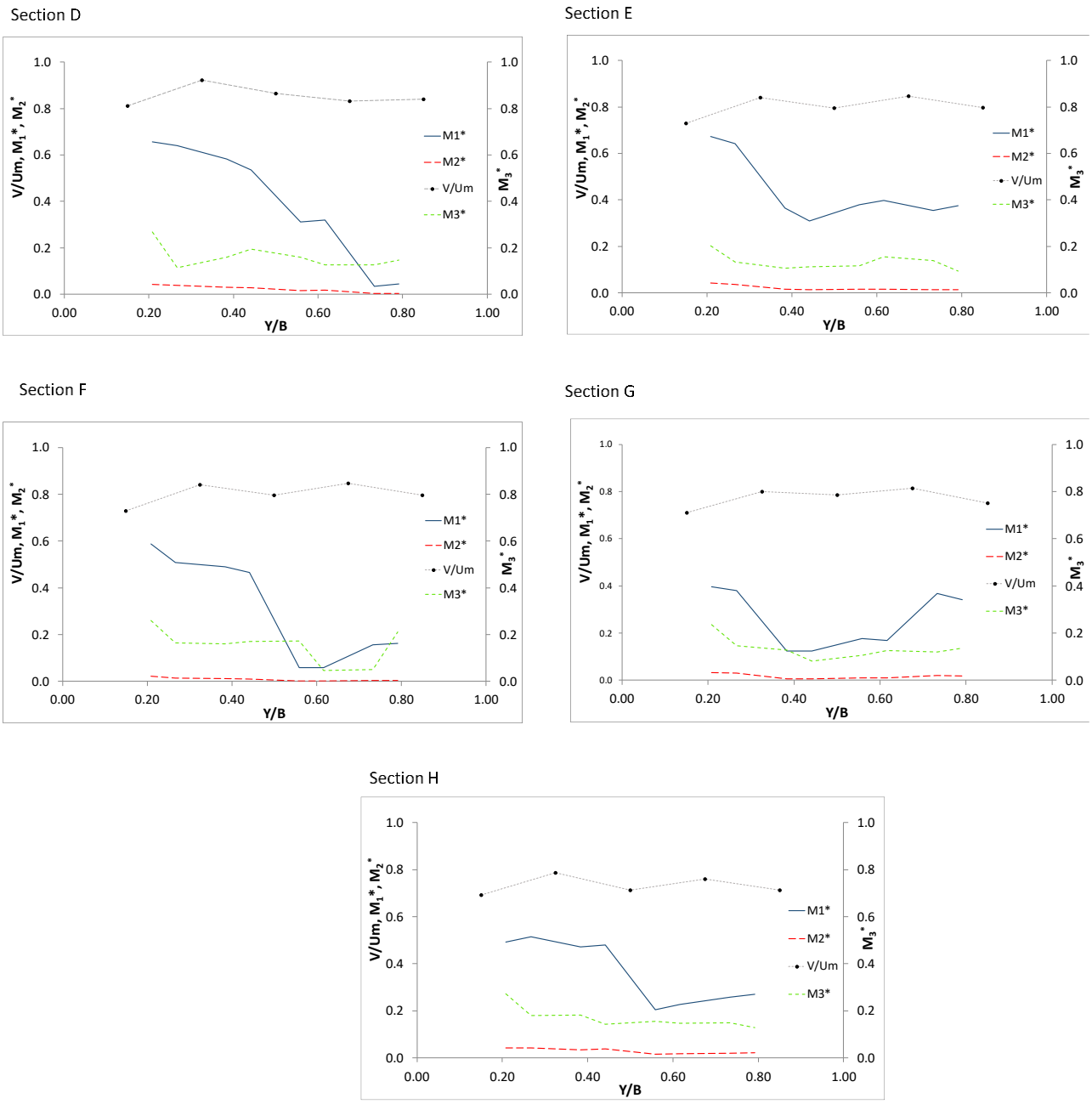

Figure 10. Comparison between the depth-averaged values of V/Um, M_1* M_2* and M_3* in sections D÷H.

4.2 Field-scale case results

Figure 11 highlights the cross-sectional distribution of the velocity at Ponte Nuovo site, along the Tiber River, under high, moderate and low flow conditions, carried out by the ADCP. The investigated cross-section exhibited larger velocity magnitudes towards the center during high and moderate flow conditions, and towards the right half during low flow conditions. With an increase in discharge, a velocity dip (the maximum velocity below the

water surface) is formed which is particularly notable in high-flow conditions (see Figure 11a). Formation of the velocity dip can be induced by various parameters, however, for the present cross-section, the aspect ratio appears to be the dominant one (Moramarco et al., 2017; Kundu and Ghoshal, 2019; Termini and Moramarco, 2020; Bahmanpouri et al., 2022a,b).

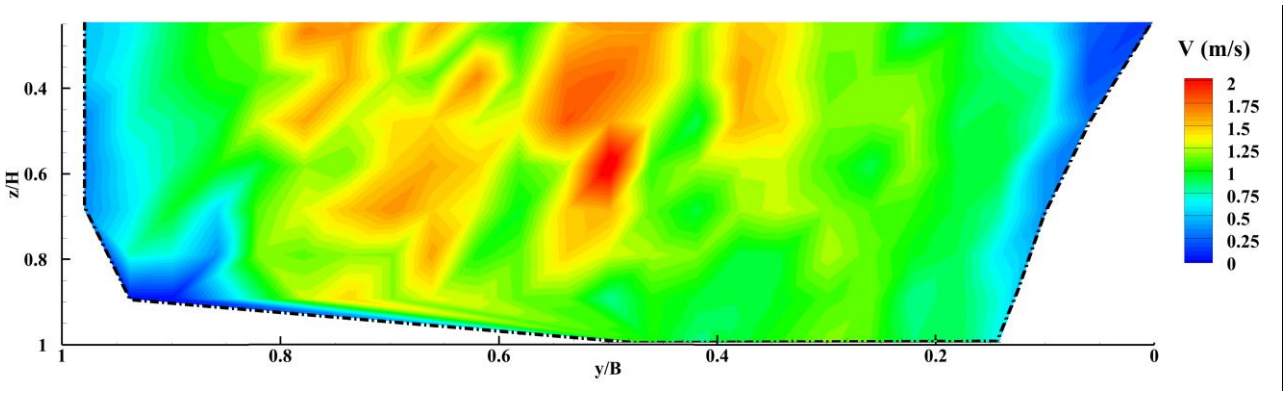

a) High flow conditions

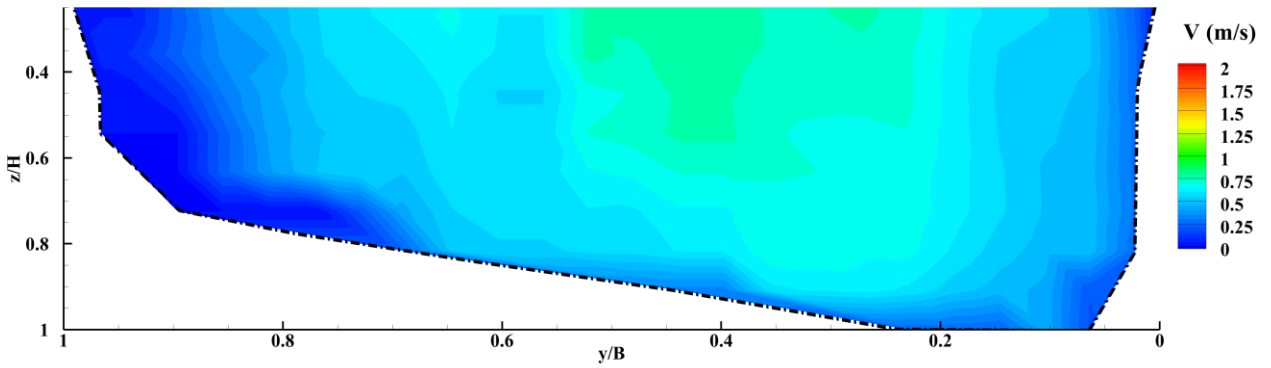

b) Moderate flow conditions

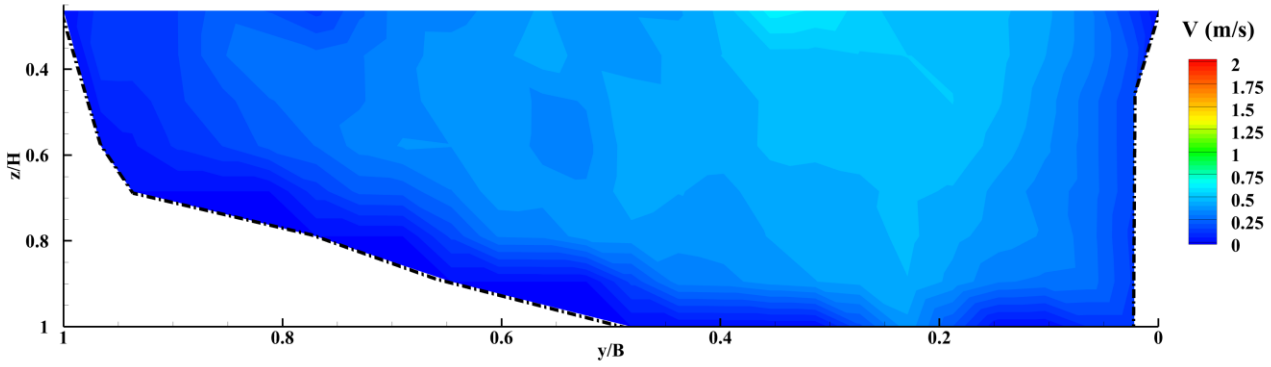

c) Low flow conditions

Figure 11. Ponte Nuovo (Tiber River): cross-sectional distribution of flow velocity for different flow conditions

Figure 12 shows the cross-sectional distribution of parameter M_1^*. For comparisons with literature, at the Ponte Nuovo section, three different scales of 0.0-0.5 J/Kg·m, 0.0-0.1 J/Kg·m and 0.0-0.04 J/Kg·m are observed under high, moderate and low flow conditions, respectively, for M_1. Notably, for all flow conditions, the larger magnitudes of parameter M_1 are associated with the larger changes of velocity magnitude in the transverse direction. Accordingly, by moving from a low-velocity region to a high-velocity region, larger magnitudes of drag force are applied to aquatic organisms. Gualtieri et al. (2017) reported the average magnitude of $0.01 < M_1$ (J/Kg.m) < 0.07 between Rio Negro and Rio Solimões in the Amazon River Basin with the $0.5 < \Delta_y$ (m) < 2.0. The kinetic energy in these flow structures can be spent by swimming fish (Videler et al. 1999; Enders et al. 2003).

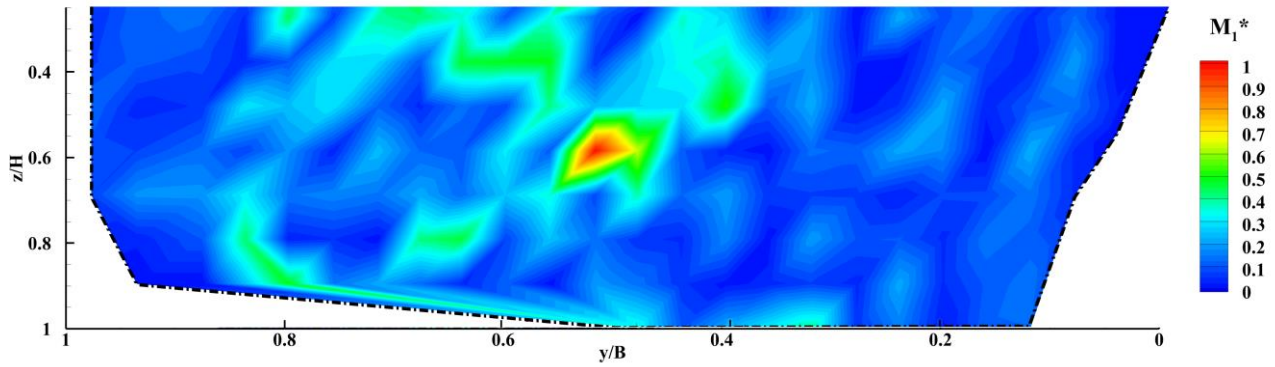

a) High flow conditions

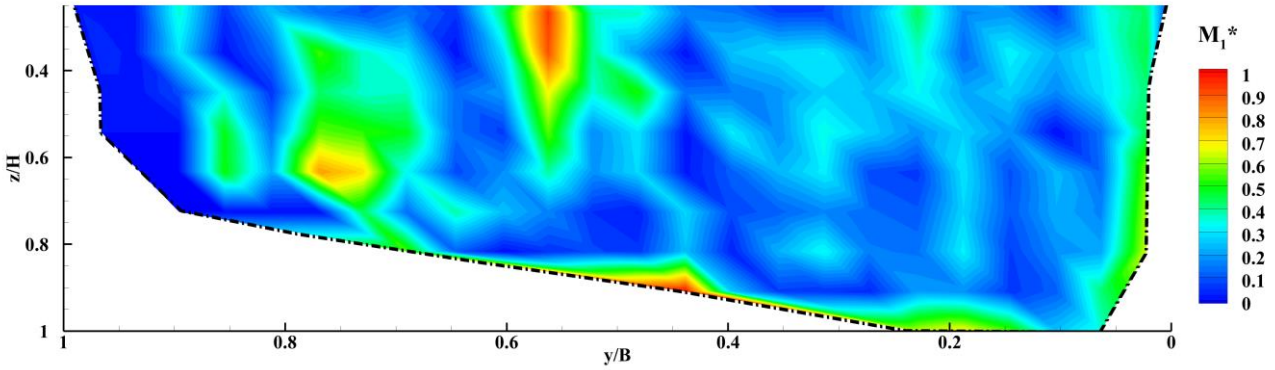

b) Moderate flow conditions

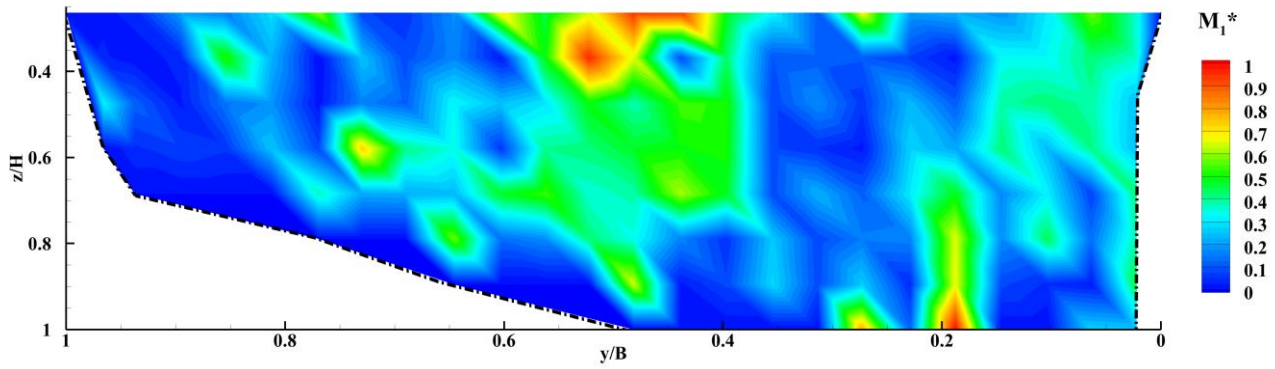

c) Low flow conditions

Figure 12. Ponte Nuovo (Tiber River): cross-sectional distribution of M_1^*

Figures 13 highlights the cross-sectional distribution of parameter M_2^* for Ponte Nuovo site. Based on parameter M_2^*, the amount of energy required for an organism to travel from a low-velocity to a high-velocity location is represented by the kinetic energy at the region with the lower velocity magnitude. Larger magnitudes of M_2^* for example at the left side of the channel for different flow conditions induced by larger changes of velocity at these zones and are induced by bed shape and bank effect.

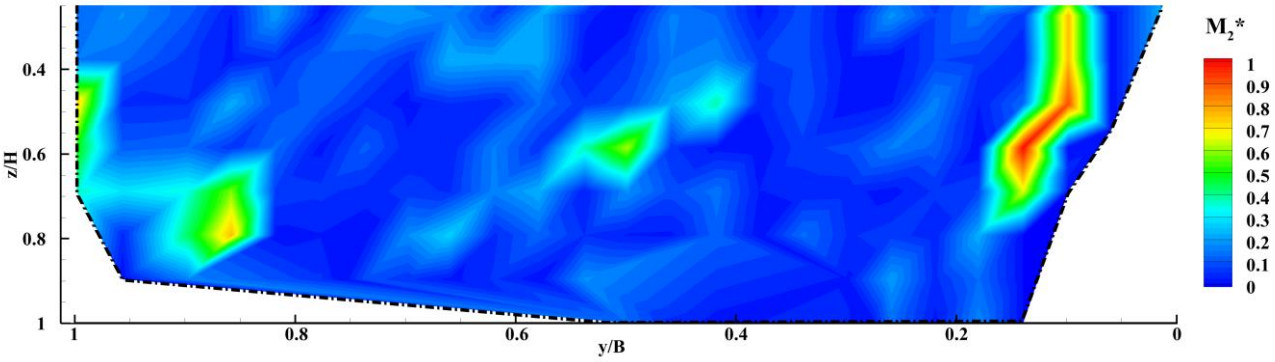

a) High flow conditions

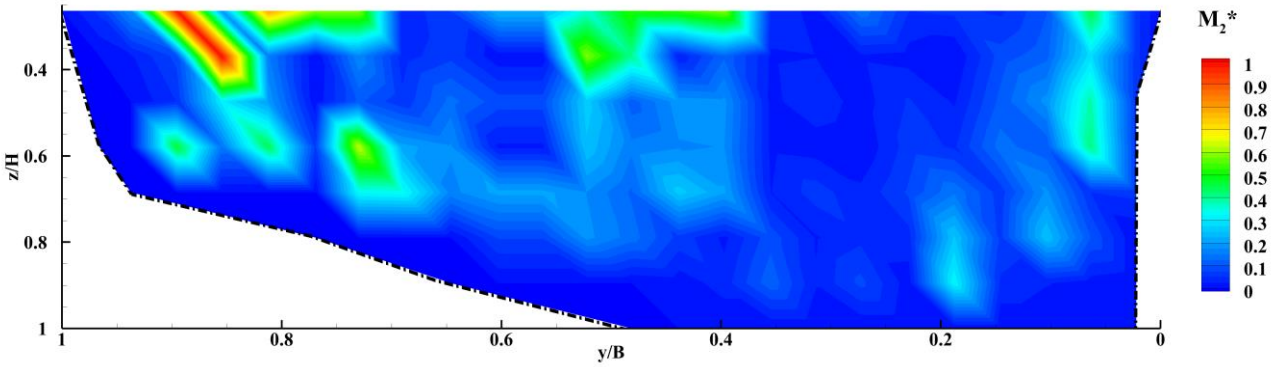

b) Moderate flow conditions

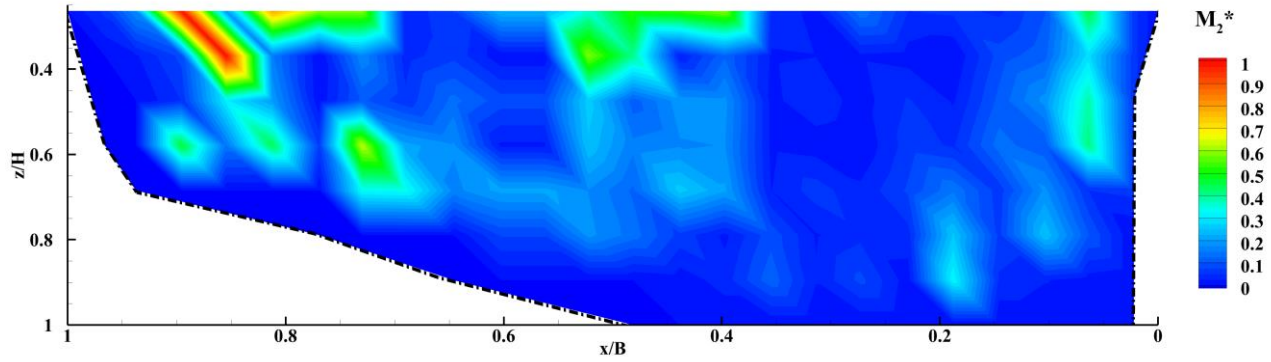

c) Low flow conditions

Figure 13. Ponte Nuovo (Tiber River): cross-sectional distribution of M_2^*

For comparisons with the literature, the minimum, average and maximum magnitudes of M_2 are equal to 0.05, 0.29, and 1.15 (1/m) under high flow, 0.04, 0.14, and 0.85 (1/m) for moderate flow, and 0.04, 0.13, and 0.75 (1/m) under low flow condition, respectively. Gualtieri et al. (2017) documented the average magnitude of $0.09 < M_2$ (1/m) < 0.37 at the confluence between Rio Negro and Rio Solimoes in the Amazon River Basin. Other researchers calculated the minimum and maximum magnitudes of M_2 as 0.08 and 0.34 (1/m) (Fausch and White, 1981), 3.1 and 40.7(1/m) (Hayes and Jowett, 1994) and 0.002 and 97.3 (1/m) (Crowder and Diplas, 2000). The value of M_2 is influenced by the characteristics of the river, including its discharge and shape, which affect the flow velocity. In case of decreasing the flow discharge such as during dry seasons or existing obstacles that cause drag like rough surfaces or bedforms, the M_2 metric would increase because the velocity in the denominator decreases.

Figures 14 shows the cross-sectional distribution of the parameter M_3^* at Ponte Nuovo station based on available observational data. Their magnitudes are similar to those by Gualtieri et al. (2020) for the low-flow condition through the Amazon River. Larger magnitudes of parameter M_3^* are observed at the whole channel for the high flow conditions, and at the sides for low and moderate flow conditions, indicating larger rates of flow circulations in these areas. This could be due to the bed profile shape observed in the Ponte Nuovo cross-section that can result in the formation of secondary currents and flow circulations.

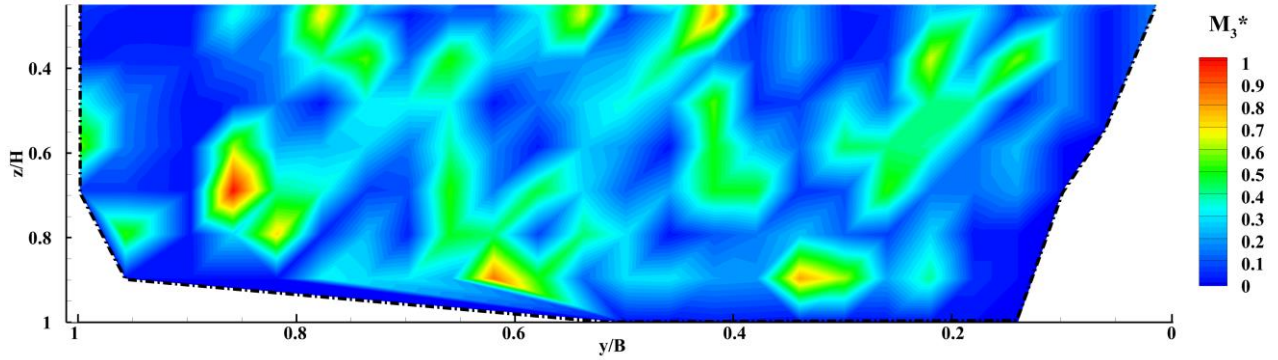

a) High flow conditions

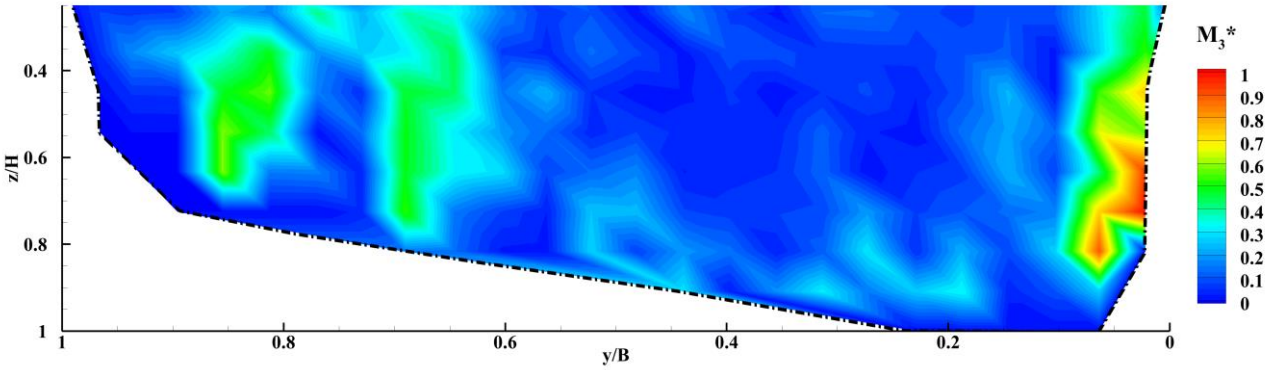

b) Moderate flow conditions

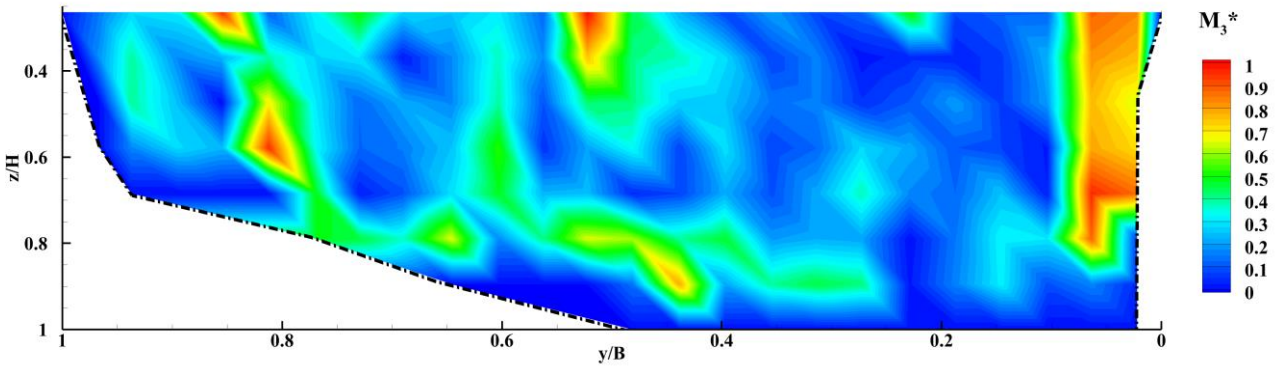

c) Low flow conditions

Figure 14. Ponte Nuovo (Tiber River): cross-sectional distribution of parameter M_3^*

The distribution of the depth-averaged values of M_1^*, M_2^* and M_3^* and the velocity ratio is illustrated in Figure 15 for all flow conditions. The parameter M_1^* is associated with the change in velocity, such that higher values of M_1^* corresponded to higher flow velocity gradients. The magnitude of the parameter M_1^* is observed to be highest at the center of the channel for all flow conditions, with a maximum value of 0.5.

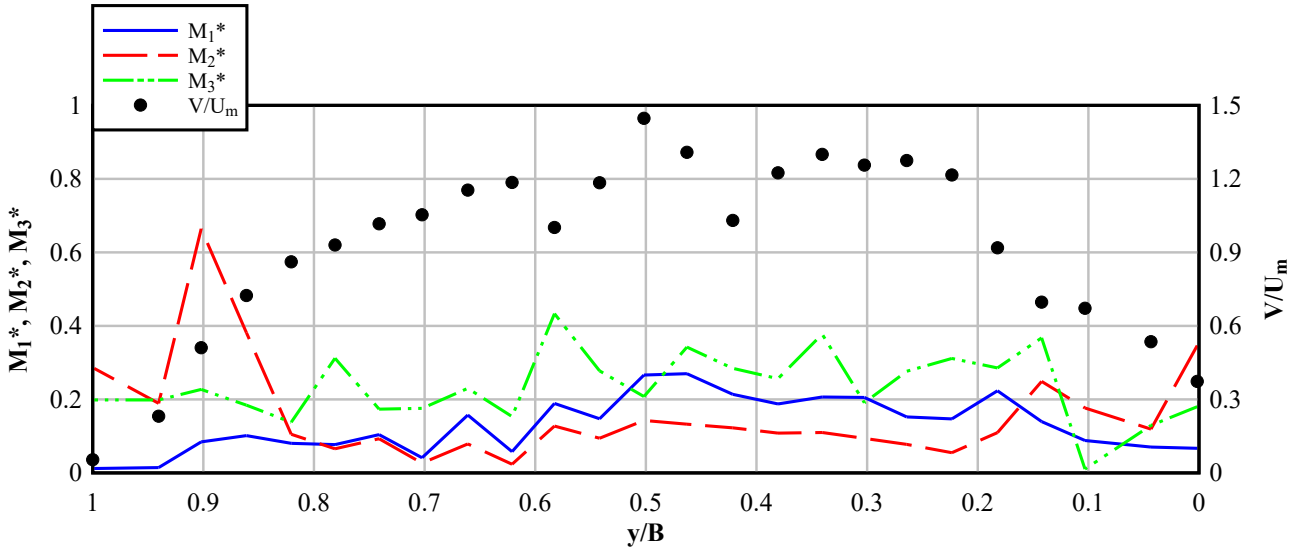

a) High flow conditions

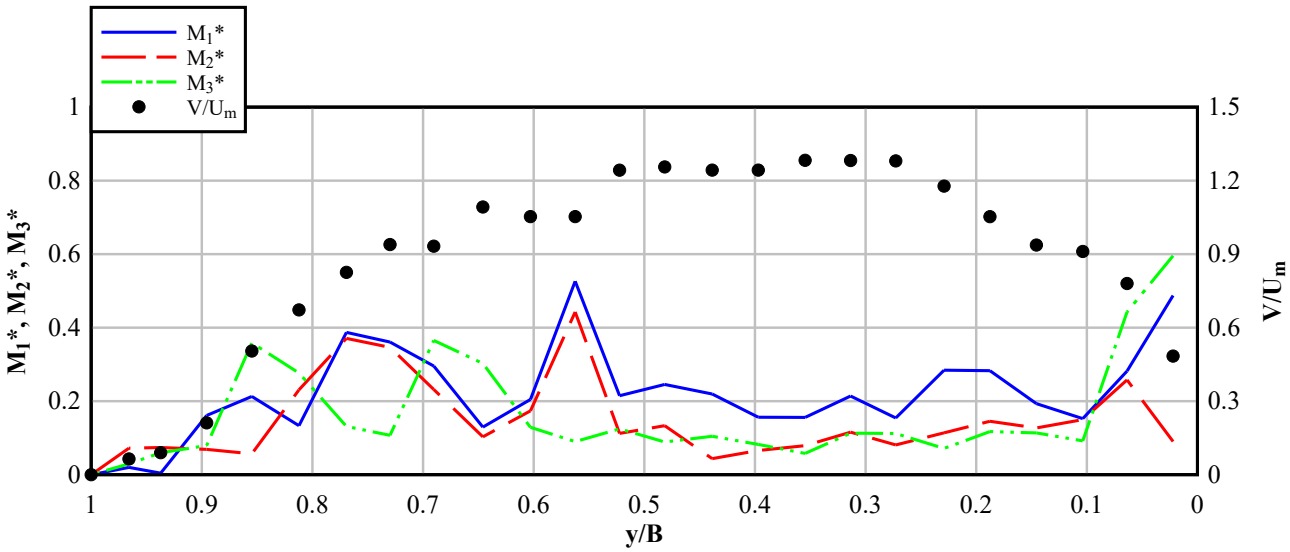

b) Moderate flow conditions

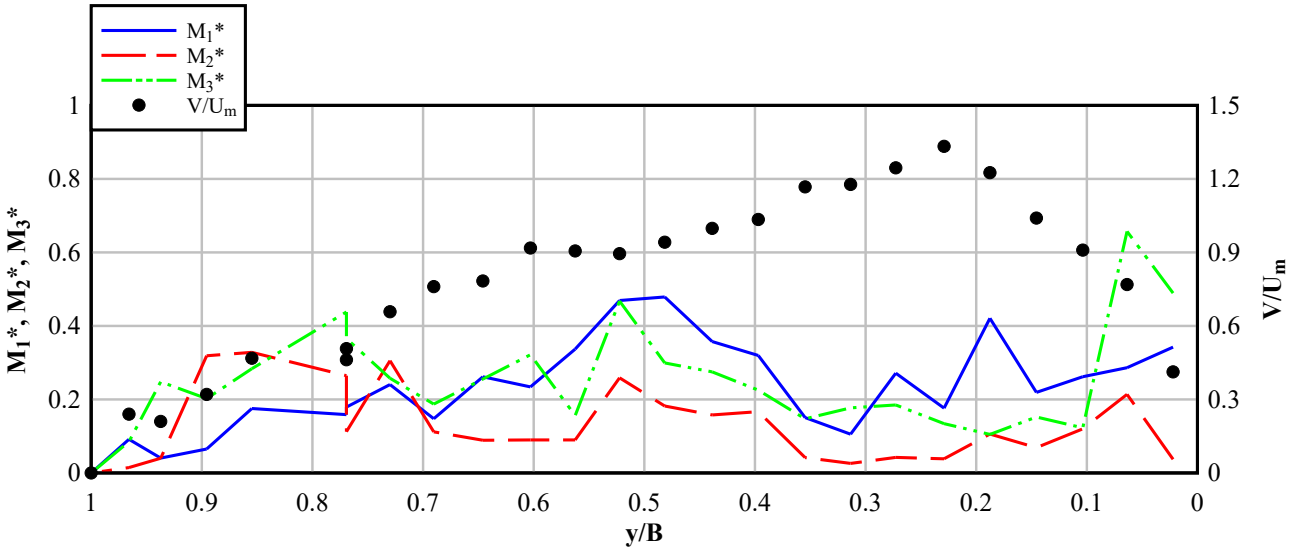

c) Low flow conditions

Figure 15. Distribution of depth-averaged M_1^*, M_2^* and M_3^* together with velocity ratio, Ponte Nuovo, Tiber River.

Furthermore, the parameter M_2* exhibited larger magnitudes on the sides of the channel for moderate flow condition and on the right side for low and high flow conditions. In high-flow conditions, the magnitudes are particularly prominent. Parameter M_3* remained nearly constant across the transverse direction in the high-flow condition. However, it is larger on the channel sides under low and medium flow conditions. It is important to note that these parameters are normalized with respect to U_m (mean velocity). For instance, in the high-flow condition, the magnitude of U_m (1.09 m/s) is greater compared to that of medium and low flow conditions (0.55 m/s and 0.34 m/s, respectively).

Discussion

The results obtained both from laboratory and field data highlight that the parameters M_1 and M_2 are strongly related to the formation of high/low velocity areas, and to the consequent accelerated-decelerated zones. By using laboratory data, high values of M_2 are found in the zones where scour holes form. The variation of the parameters, especially M_2, is linked to the kinetic energy of the flow. This is especially important, as an example, in locally accelerated stream-wise velocity around obstructions, such as piers, which thus provide favorable migration corridors for fishes determining mean velocities that are greater than average reach velocities with low relative turbulence (Tritico and Hotchkiss 2005). The lowest achievable value of M_2 for each zone would occur if the mildest velocity gradient surrounded the location of an aquatic organism. Conversely, the highest attainable value would be reached when the steepest change in velocity is found at the location. Shields et al. (1995) based on the placement of spur dikes, which create vortices, substantially increased fish biomass in river flow. Their results reasoned that before attempting to restore the physical habitat, it is important to ensure that the water quality in terms of suspended particles is good enough to sustain aquatic life. The range of above parameters suggest the

same flow patterns that may indicate suitable habitats for the organisms such as fishes. Based on previous research works (e.g. Gualtieri et al., 2017, 2019), the difference in parameters values could be both because of different directions and distances between the velocity magnitudes. Furthermore, the varying flow kinematic conditions made it challenging to make a comprehensive comparison. Kozarek et al. (2010) based on field data on Staunton River, Canada, reported that, although velocity or depth characteristics are insufficient to explain fish (brook trout) habitat preferences in the complex flows created by boulders and other flow obstructions, brook trout density generally increased as the flow complexity increased. The finding was in agree with the anticipated behavior of piscivorous species, which tend to exhibit a preference for positions in close proximity to regions characterized by high gradients. Such a strategic placement allows these species to conserve energy in slow-flowing areas while still benefiting from access to fast-moving currents for prey acquisition (Nestler et al., 2012; Liao, 2007; Booker et al., 2004). In the case of field observations, it was found that freshwater dolphins in the confluence of the Negro and Solimões Rivers actively avoided areas with high M_2 values (Gualtieri et al., 2017, 2020).

Vorticity is a potentially useful metric for calculating spatial flow patterns for biological purposes (Crowder and Diplas 2002). The parameter M_3 based on velocity components indicate the strength of rotation in the flow domain that can be applied to identify preferred spawning grounds for fish (Yang et al., 2008; Zhu et al., 2013). The laboratory data show that M_3 higher values of circulation are found close to the front deposit and in the scour holes, i.e. especially where the bed profile changes. Thus, the obtained results suggest that the animal should spend more energy where the erosion process on the bed develops until the formation of the scour hole. Larger magnitudes of parameter M_3 are also observed, under high and moderate flow conditions, close to the banks due to the deformed bed profile observed in the Ponte Nuovo cross-section, resulting in the formation of secondary

currents and flow circulations. These findings confirm the observations reported by previous researchers. Bedulli et al., (1990) reported that the total density of aquatic organisms such as zoobenthos decreased during the low flow condition in the summer months with respect to the preceding years. However, in samples collected in the late spring, Ferrari and Rossetti (1990) observed a notable increase in the numerical importance of aquatic organisms such as phytal copepods and gastropod larvae.

Some researchers defined a synthetic parameter, the mean individual size (B/A), i.e. the ratio between total biomass (B) and total abundance (A) of organisms to describe the disturbance effects on the community. Such a ratio tends to diminish progressively along a gradient of increasing organic enrichment of sediment (Pearson and Rosenberg, 1978; Weston, 1990, Ceccherelli et al. 1994). Therefore, it is thought that the zones with high vorticities are potential zones for deposited sediment particles. Consequently, these zones can be considered as potential zones for feeding aquatic organisms. Table 2 compares the minimum, average, and maximum magnitudes of hydraulic complexity parameters for the present research and the available data from the literature.

Table 2. Minimum, averaged, and maximum magnitudes of hydraulic complexity parameters

Study and data type	**M_1 (J/Kg.m)**			**M_2 (1/m)**			**M_3 (1/s)**		
	Min	Ave.	Max	Min	Ave.	Max	Min	Ave.	Max
Present research-Laboratory	0.0002	0.06	0.249	0. 6	119.13	500.88	0.0002	0.06	0.249
Present research – Field – Low flow	0.001	0.01	0.04	0.05	0.29	1.15	0.001	0.10	0.39
Present research – Field – Medium flow	0.001	0.01	0.02	0.04	0.14	0.85	0.001	0.06	0.36
Present research – Field – High flow	0.001	0.13	0.92	0.04	0.13	0.75	0.001	0.07	0.50
Fausch and White, (1981) - Field	-	-	-	0.08	-	0.34	-	-	-
Hayes and Jowett,	-	-	-	3.1	-	40.7	-	-	-

(1994) - Field									
Crowder and Diplas, (2000) - Laboratory	-	-	-	0.002	-	97.3	-	-	-
Gualtieri et al., (2017, 2019) - Field	0.01	-	0.07	0.09	-	0.037	0.047	-	0.055
Glopira et al., (2022) - Laboratory	0.001	0.38	1.6	0.001	4.56	52.61	-	-	-

In terms of the cross-sectional distribution of hydraulic complexity parameters, generally, M_1 has an inverse relationship with M_2 and M_3 so that large magnitudes of M_1 are observed at the center of the cross-section while large magnitudes of M_2 and M_3 are seen bear the banks. In terms of depth-averaged distribution of hydraulic complexity parameters, overall, all parameters have the same trend of changing the magnitude in the transverse direction. It means a change in kinetic energy of flow in transverse direction may result in the formation of circulations in flow.

Vortices generated by the movement of a fish's fins play a part in determining a fish's maneuverability (Bandyopadhyay et al. 2000). Piscivorous predators and copepods can detect the presence of prey through the vortex structures left behind by fish and other organisms as they swim (Hanke et al. 2000). Way et al. (1995) found that grooved blocks used to line parts of the Mississippi River created small eddies that allow macroinvertebrates to build feeding structures that are sheltered from high-velocity flows but remained in contact with faster feeding flows. Herein, larger circulations are observed at the bank sides or bottom of the cross-section due to larger vertical-averaged velocity differences. Crowder and Diplas (2002) reported relatively high vorticities along the channel banks. Such observations suggest that aquatic organisms use vortices and other complex flows in different manners and at different scales.

Conclusions

Flow patterns, such as changes in velocity, recirculation zones, and flows perpendicular to the main current, are usually caused by the presence of mesoscale topographical features. These flow patterns have a significant impact on stream ecology. The hydraulic complexity metrics known as M_1, M_2, and M_3 are investigated for the velocity dataset collected at the laboratory as well as Ponte Nuovo gauged site, along the Tiber River in Italy. In this direction, the velocity components measured in selected cross-sections are used. In terms of ecological function, these parameters are of particular significance for analysing habitat metrics in 3D space. The M_1 and M_2 parameters provides an estimation of the kinetic energy spent by organisms in the flow to move. Flow circulation is highlighted by the M_3 parameter, indicating that the areas with flow circulation are not considered as the primary habitats for aquatic organisms. However, these areas could serve as potential feeding grounds for aquatic organisms. Based on the laboratory data, the results demonstrate that the parameters, particularly M_3, effectively characterized the variation in flow velocity and the impact resulting from the development of turbulent structures and flow circulation within each cross-section. These parameters are strongly correlated with the formation of scour holes and deposit fronts. The obtained patterns of the stream parameters suggest that the animal should spend more energy where the erosion process develops on the bed until the formation of the scour hole. In these areas, flow circulation assumes also high values influencing the animal's activities. The application of field data indicates that larger magnitudes of M_3 are observed at different parts of the cross-section, especially near banks, depending on flow type allowing the detection of larger flow circulations zones. Overall, parameter M_1 has an inverse direction with the parameters M_2 and M_3 as larger magnitudes of M_1 are observed at the centre of cross-section while large magnitudes of M_2 and M_3 are seen near the banks.

Generally, the results highlight the possibility to detect potential locations for a larger density of aquatic organisms. Overall, the findings suggest that the hydraulic complexity

parameters might add some insights into the habitat heterogeneity as well as evaluate ecological and biological patterns in rivers with remarkable flood rates such as Tiber River.

Acknowledgments

This work has been supported by Italian National Research Programme PRIN 2017, with the project "*IntEractions between hydrodyNamics flows and bioTic communities in fluvial Ecosystems: advancement in dischaRge monitoring and understanding of Processes Relevant for ecosystem sustaInability by the development of novel technologies with fIeld observatioNs and laboratory testinG* (ENTERPRISING)". The first author dedicates this work to the memory of his uncle, Amirhamzeh Bahmanpouri.

REFERENCES

Bahmanpouri, F., Barbetta, S., Gualtieri, C., Ianniruberto, M., Filizola, N., Termini, D., Moramarco, T., 2022a. Prediction of river discharges at confluences based on Entropy theory and surface-velocity measurements. J. Hydrol., 127404. https://doi.org/10.1016/j.jhydrol.2021.127404.

Bahmanpouri, F., Eltner, A., Barbetta, S., Bertalan, L., Moramarco, T., 2022b. Estimating the average river cross section velocity by observing only one surface velocity value and calibrating the entropic parameter. Water Resour. Res., https://doi.org/10.1029/2021WR031821.

Bahmanpouri, F., Termini, D., Barbetta, S., Dionigi, M., Moramarco, T., 2023. Significance of hydraulic complexity parameters M1 and M2 based on laboratory and field data. Hydrol. Res. 2023; nh2023089. doi: https://doi.org/10.2166/nh.2023.089

Bandyopadhyay, P.R., Castano, J.M., Nedderman, W.H., Donnelly, M.J., 2000. Experimental simulation of fish-inspired unsteady vortex dynamics on a rigid cylinder. J. Fluids Eng. Trans. ASME, 122: 219–238.

Bedulli D., Pugnetti A., Ferrari I., 1990. Evoluzione recente deipopolamenti zoobentonici e zooplanctonici in una laguna del Delta del Po. Oebalia, 16: 103-111.

Blackburn J, Steffler P., 2002. River2d two-dimensional depth averaged model of river hydrodynamics and fish habitat: river2d tutorial—the basics. Accessed: July 2004.

Blettler, M.C.M., Amsler, M.L., Ezcurra De Drago, I., Drago, E., Paira, A., Espinola, L.A., … and Szupiany, R., 2016. Fine sediment input and benthic fauna interactions at the confluence of two large rivers. Int. J. Environ. Res., 10(1), 65–76.

600 Booker, D.J., Dunbar, M.J., Ibbotson, A., 2004. Predicting juvenile salmonid drift-feeding habitat quality using
601 a three-dimensional hydraulic-bioenergetic model. Ecol. Model. 177, 157–177.
602 https://doi.org/10.1016/j.ecolmodel.2004.02.006
603 Ceccherelli, V.U., Ferrari, I., Viaroli, P., 1994. Ecological research on the animal communities of the Po River
604 Delta lagoons.
605 Clark, J.S., Rizzo, D.M., Watzin, M.C., Hession, W.C., 2008. Spatial distribution and geomorphic condition of
606 fish habitat in streams: an analysis using hydraulic modelling and geostatistics. River Res. Appl., 24(7),
607 885-899.
608 Crowder, D. W., Diplas, P., 2000. Evaluating spatially explicit metrics of stream energy gradients using
609 hydrodynamic model simulations. Can. J. Fish. Aquat. Sci., 57(7), 1497-1507.
610 Crowder, D.W., Diplas, P., 2002. Vorticity and circulation: Spatial metrics for evaluating flow complexity in
611 stream habitats. J. Fish. Aquat. Sci., (JFAS), 59(4), 633–645.
612 Enders, E.C., Boisclair, D., Roy, A.G., 2003. The effect of turbulence on the cost of swimming for juvenile
613 Atlantic salmon (Salmosalar). J. Fish. Aquat. Sci., (JFAS), 60(9), 1149–1160.
614 Fausch, K.D., White, R.J., 1981. Competition between brook trout (Salvelinus fontinalis) and brown trout
615 (Salmo trutta) for position in a Michigan stream. Can. J. Fish. Aquat. Sci. 38: 1220–1227.
616 Ferrari I., Rossetti G., 1990. Zooplankton in the Po River Delta (terminal reach of the Po di Pila, Sacca del
617 Canarin and nearby sea): a synthesis of research carried out from 1977 to 1988. In: ENEL-SIBM
618 Symposium on the ecology of the Po River Delta. Collected Contributions. Vol. 2, Contribution No. 12, 37
619 pp.
620 Golpira, A., Baki, A.B., Ghamry, H., Katopodis, C., Withers, J., Minkoff, D., 2022. An experimental study:
621 effects of boulder placement on hydraulic metrics of instream habitat complexity. Sci. Rep., 12(1), 13156.
622 Gualtieri, C., Abdi, R., Ianniruberto, M., Filizola, N., Endreny, T.A., 2020. A 3D analysis of spatial habitat
623 metrics about the confluence of Negro and Solimões rivers, Brazil. Ecohydrol., 13(1), e2166.
624 Gualtieri, C., Ianniruberto, M., Filizola, N., Santos, R., Endreny, T., 2017. Hydraulic complexity at a large river
625 confluence in the Amazon basin. Ecohydrol., 10(7), e1863.
626 Hanke, W., Brucker, C., Bleckmann, H., 2000. The ageing of the low-frequency water disturbances caused by
627 swimming foldfish and its possible relevance to prey detection. J. Exp. Biol. 203:1193–1200.
628 Hayes, J.W., Jowett, I.G., 1994. Microhabitat models of large drift-feeding brown trout in three New Zealand
629 rivers. N. Am. J. Fish. Manag., 14(4), 710–725.
630 Irfan, S., Alatawi, A.M.M., 2019. Aquatic ecosystem and biodiversity: a review. Open J. Ecol., 9(1), 1-13.

631 J. Morin, P., McGrady-Steed, J., 2004. Biodiversity and ecosystem functioning in aquatic microbial systems: a
632 new analysis of temporal variation and species richness-predictability relations. Oikos, 104(3), 458-466.
633 Kozarek, J., Hession, W., Dolloff, C., Diplas, P., 2010. Hydraulic complexity metrics for evaluating in-stream
634 brook trout habitat. J. Hydraul. Eng., 136 (12): 1067-1076, 136(12), 1067-1076.
635 Kundu, S., Ghoshal, K., 2019. An Entropy Based Model for Velocity-Dip-Position. J. Environ. Inform. 33 (2),
636 113-128.
637 Liao, J.C., 2007. A review of fish swimming mechanics and behaviour in altered flows. Philos. Trans. R. Soc.
638 B Biol. Sci. 362, 1973–1993. https://doi.org/10.1098/rstb.2007.2082
639 Maddock, I., 1999. The importance of physical habitat assessment for evaluating river health. Freshw. Biol.,
640 41(2), 373–391.
641 Moramarco, T., Barbetta, S., Tarpanelli, A., 2017. From surface flow velocity measurements to discharge
642 assessment by the entropy theory. Water, 9(2), 120.
643 Munson, B.R., Young, D.F., Okiishi, T.H., 1990. Fundamentals of fluid mechanics. 2nd ed., John Wiley and
644 Sons, Inc., New York.
645 Nepf, H., Puijalon, S., Capra, H., 2022. Organism-scale interaction with hydraulic conditions. J. Ecohydraul.,
646 7(1), 1-3.
647 Nestler, J.M., Pompeu, P.S., Goodwin, R.A., Smith, D.L., Silva, L.G.M., Baigún, C.R.M., Oldani, N.O., 2012.
648 The River Machine: A Template for Fish Movement and Habitat, Fluvial Geomorphology, Fluid Dynamics
649 and Biogeochemical Cycling. River Res. Appl. 28, 490–503. https://doi.org/10.1002/rra.1567
650 Pearson T.H., Rosenberg R., 1978. Macrobenthic succession in relation to organic enrichment and pollution of
651 the marine environment. Oceanogr. Mar. Biol.: An Annual Review, 16: 229-311.
652 Pedersen, M.L., Friberg, N., Larsen, S.E., 2004. Physical habitat structure in Danish lowland streams. River
653 Res. Appl ., 20(6), 653-669.
654 Protasov, A., Barinova, S., Novoselova, T., Sylaieva, A., 2019. The aquatic organisms diversity, community
655 structure, and environmental conditions. Diversity, 11(10), 190.
656 Rempel, L.L., Richardson, J.S., Healey, M.C., 1999. Flow refugia for benthic macroinvertebrates during
657 flooding of a large river. J. North Am. Benthol. Soc., 18(1), 34–48.
658 Shields, F.D., Jr., Cooper, C.M., Knight, S.S., 1995. Experiment in stream restoration. J. Hydraul. Eng.
659 (ASCE),121: 494–502.
660 Shields, F.D., Rigby, J.R., 2005. River habitat quality from river velocities measured using acoustic Doppler
661 current profiler. Environ. Manage. (N.Y.), 36(4), 565–575.

662 Smith, D.L., Brannon, E.L., Shafii, B., Odeh, M., 2006. Use of the average and fluctuating velocity components
663 for estimation of volitional rainbow trout density. Trans. Am. Fish. Soc., 135(2), 431–441.
664 Termini D., 2015. Experimental Analysis of Horizontal Turbulence of Flow over Flat and Deformed Beds. Arch.
665 Hydroengineering Environ., Volume 63, Issue 3-4, pp. 77–99.doi10.1515/heem-2015-0021
666 Termini D., Moramarco T., 2020. Entropic model application to identify cross-sectional flow effect on velocity
667 distribution in a large amplitude meandering channel. Adv. Water Resour., vol. 143,
668 https://doi.org/10.1016/j.advwatres.2020.103678.
669 Termini, D., Sammartano, V., 2008. Experimental analysis of relations between coherent turbulent
670 structures and formation of bedforms. Arch. Hydroengineering Environ., 55(3-4), 125-143.
671 Tritico, H.M., Hotchkiss, R.H., 2005. Unobstructed and obstructed turbulent flow in gravel bed rivers. J. Hydrol.
672 Eng., 131(8), 635–645.
673 Videler, J.J., Muller, U.K., Stamhuis, E.J., 1999. Aquatic verte-brate locomotion: Wakes from body waves. J.
674 Exp. Biol. 202(23),3423–3430.
675 Way, C.M., Burky, A.J., Bingham, C.R., Miller, A.C., 1995. Substrate roughness, velocity refuges, and
676 macroinvertebrate abundance on artificial substrates in the lower Mississippi River. J. North Am. Benthol.
677 Soc.. 14: 510–518.
678 Weston D. P., 1990. Quantitative examination of microbenthic community changes along an enrichment
679 gradient. Mar. Ecol. Prog. Ser., 61: 233-244.
680 Yang, Y., Yan, Z., Chang, J., 2008. Hydrodynamic characteristics of Chinese sturgeon spawning ground in
681 Yangtze River. J. Hydrodynam., 20(2), 225–230.
682 Zhu, Z.W., Wang, S.Q., Duan, X.B., Luo, H.W., Chen, D.Q., Sun, M.S., … Yu, L.X., 2013. Studying the
683 variation of cross-section vorticity on the spawning grounds of the four major Chinese carps in the middle
684 reach of the Yangtze River. J. Appl. Ichthyol., 29, 1463–1467.
685
686